Nanosemiconductor-Based Photocatalytic Vapor Generation Systems for Subsequent Selenium Determination and Speciation with Atomic Fluorescence Spectrometry and Inductively Coupled P...

ARTICLE *in* ANALYTICAL CHEMISTRY · FEBRUARY 2012

Impact Factor: 5.64 · DOI: 10.1021/ac3001995 · Source: PubMed

5 AUTHORS, INCLUDING:

Yacui Luo
Xiamen University
5 PUBLICATIONS **83** CITATIONS
SEE PROFILE

Zhaoxin Li
Teachers College
7 PUBLICATIONS **93** CITATIONS
SEE PROFILE

Qiuquan Wang
Xiamen University
80 PUBLICATIONS **1,163** CITATIONS
SEE PROFILE

analytical chemistry

Article

pubs.acs.org/ac

Nanosemiconductor-Based Photocatalytic Vapor Generation Systems for Subsequent Selenium Determination and Speciation with Atomic Fluorescence Spectrometry and Inductively Coupled Plasma Mass Spectrometry

Huamin Li,[†] Yacui Luo,[†] Zhaoxin Li,[†] Limin Yang,[†] and Qiuquan Wang*[,†,‡]

[†]Department of Chemistry and the Key Laboratory of Analytical Sciences, College of Chemistry and Chemical Engineering, and [‡]State Key Laboratory of Marine Environmental Science, Xiamen University, Xiamen 361005, China

Supporting Information

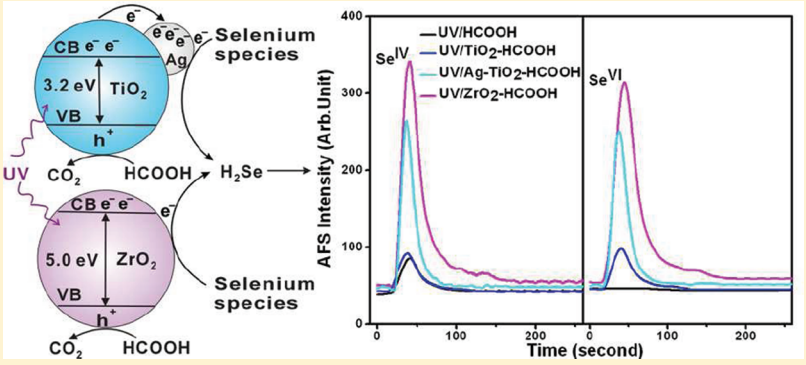

ABSTRACT: We reported novel Ag−TiO_2- and ZrO_2-based photocatalytic vapor generation (PCVG) systems as effective sample introduction techniques for further improving the sensitivity of the atomic spectrometric determination of selenium for the first time, in which the conduction band electron served as a "reductant" to reduce selenium species including Se^{VI} and convert them directly into volatile H_2Se, which was easily separated from the sample matrix and underwent more effectively subsequent atomization and/or ionization. These two PCVG systems helped us to overcome the problem encountered in the most conventional KBH_4/OH^--H^+ system, in that Se^{VI} was hardly converted into volatile selenium species without the aid of prereduction procedures. The limits of detection (LODs) (3σ) of the four most typical Se^{IV}, Se^{VI}, selenocystine ($(SeCys)_2$), and selenomethionine (SeMet) species were, respectively, down to 1.2, 1.8, 7.4, and 0.9 ng mL^{-1} in UV/Ag−TiO_2−HCOOH, and 0.7, 1.0, 4.2, and 0.5 ng mL^{-1} in UV/ZrO_2−HCOOH with the relative standard deviations (RSDs) lower than 5.1% (n = 9 at 1 μg mL^{-1}) when using atomic fluorescence spectrometry (AFS) under flow injection mode. They reached 10, 14, 18, and 8 pg mL^{-1} in UV/Ag−TiO_2−HCOOH, and 6, 7, 10, and 5 pg mL^{-1} in UV/ZrO_2−HCOOH with the RSDs lower than 4.4% (n = 9 at 10 ng mL^{-1}) when using inductively coupled plasma mass spectrometry (ICPMS). After the two PCVG systems were validated using certified reference materials GBW(E)080395 and SELM-1, they were applied to determine the total Se in the selenium-enriched yeast sample and used as interfaces between high-performance liquid chromatography (HPLC) and AFS or ICPMS for selenium speciation in the water- and/or enzyme-extractable fractions of the selenium-enriched yeast.

Tracing back to the development of analytical atomic spectrometry including atomic emission spectrometry, atomic absorption spectrometry (AAS), and atomic fluorescence spectrometry (AFS) as well as inductively coupled plasma mass spectrometry (ICPMS), a suitable sample introduction system is crucial, since it is responsible significantly for the method sensitivity when the hardware for the atomization and/or ionization as well as spectrometric determination of target elements is fixed. In comparison with the conventional nebulization system, in which the sample introduction efficiency is less than 5% in general, leading to a 95% loss of method sensitivity, hydride generation (HG), a more efficient sample introduction system, was first introduced in 1969, in which a Zn−acid system was developed and used as a sample introduction system for generating AsH_3 followed by AAS determination, greatly changing and improving the situation of analytical atomic spectrometry in terms of sensitivity.[1] This pioneer work triggered the later developments of HG using tetrahydroborate (THB) instead of Zn−acid to reduce not only As but also many other elements, which can be reduced into volatile species and cold element vapor, for subsequent high-sensitivity atomic spectrometric determina-

Received: January 19, 2012
Accepted: February 13, 2012
Published: February 13, 2012

   dx.doi.org/10.1021/ac3001995 | *Anal. Chem.* 2012, 84, 2974−2981

tion.[2,3] This typical THB-HG system benefits from several merits, for example, a nearly 100% sample introduction efficiency, efficient separation of the target elements from complex sample matrix avoiding possible physicochemical and spectral interferences from coexisting elements and compounds, as well as easy atomization of the generated volatile species at an atomizer.[3] On the other hand, however, the drawbacks of THB-HG are also obvious; for example, the interference of transition metals (such as Co^{2+}, Ni^{2+}, and Fe^{2+}) and the instability of THB, and more seriously, the THB-HG efficiency is affected strongly by the existing chemical form or oxidation state of targeted elements. Considering the hypothesis of reduction in the THB-HG system, hydrogen transfer from THB and/or its reactive intermediates to the targeted elements is the fundamental mechanism.[3] The reduction processes are accompanied by "electron" (e^-) translocation to the targeted elements, and thus they are reduced into their corresponding volatile hydrides or cold elemental vapor. Following this clue, from the beginning of this century our group started to seek electron-offering systems. TiO_2–HCOOH under UV-irradiation (UV/TiO_2–HCOOH) is one of the successful systems. In this system, the e^- at the conduction band of nano-TiO_2 generated under UV irradiation is utilized to reduce different Se and Hg species into Se^0 and Hg^0, while HCOOH reacts with the oxidative hole (h^+) generated at the valence band as an h^+ scavenger.[4−6] In this case, the cold vapor Hg^0 can be directly separated via a gas−liquid phase separator and determined using AFS.[6] However, Se^0, which tends to aggregate into particles, is difficult to be separated from the liquid reaction medium and transferred into the Ar–H_2 flame (only 900 °C) for determination when using a conventional nondispersive AFS. UV/TiO_2–HCOOH served as a prereduction unit especially in the case of Se^{VI} (which cannot be converted directly into H_2Se in the typical THB-HG system) before further reduction of Se^0 by THB into H_2Se for highly efficient transfer into the Ar–H_2 flame.[4] The subsequent studies also indicated that inorganic Se species could be converted into volatile chemical species under UV/TiO_2–HCOOH when avoiding the use of phosphate buffer or using a boiled-water bath for ICPMS and AFS determination.[7,8] Almost in the same period, low molecular weight organic acids were employed to generate reductive radicals under UV irradiation, and these reductive radicals were able to reduce targeted elements into their volatile chemical species for atomic spectrometric determination although the vapor generation (VG) efficiency needs to be further improved, and it was still difficult to convert the target elements at higher oxidation states into their volatile chemical species in some cases.[9−18] These systems based on low molecular weight organic acid and/or nanosemiconductor demonstrated that the trend in sample introduction techniques for atomic spectrometry is developing to simpler, greener, and more efficient ways.[19]

Here, we reported two new ways in order to further improve the nanosemiconductor-based photocatalytic VG (PCVG) efficiency allowing direct VG of not only selenite (Se^{IV}) and organic Se species such as selenomethionine (SeMet) and selenocystine ($(SeCys)_2$) but also selenate (Se^{VI}) for higher sensitivity atomic spectrometric determination. One way was to load noble metal nanoparticles onto the surface of nano-TiO_2 in order to prevent the rapid recombination of e^-/h^+ pairs, moving the Fermi level of nano-TiO_2 to a more negative potential due to the increase of e^- accumulation at the conduction band and thus resulting in a higher e^- density for the PCVG; the other was to use nano-ZrO_2, which has a large energy gap (5.0 eV greater than that (3.2 eV) of nano-TiO_2) between the conduction band and valence band, to obtain a conduction band e^- of more negative potential and thus stronger reductivity. These two nanosemiconductor-based PCVG systems together with AFS and/or ICPMS were applied to Se determination and further used as interfaces between high-performance liquid chromatography (HPLC) and AFS and/or ICPMS for Se speciation analysis in the extracts of selenium-enriched yeast.

EXPERIMENTAL SECTION

Chemicals. All reagents used were at least of analytical grade. Ultrapure water (UPW, 18.2 MΩ cm) was prepared in a Milli-Q system (Millipore Filter Co., Bedford, U.S.A.) and used throughout this study. Tetrabutyl titanate ($Ti(OC_4H_9)_4$), tetrapropyl zirconate ($Zr(OC_3H_7)_4$), silver nitrate ($AgNO_3$), hydrogen tetrachloroaurate trihydrate ($HAuCl_4{\cdot}3H_2O$), hydrogen hexachloroplatinate hexahydrate ($H_2PtCl_6{\cdot}6H_2O$), oxalic acid ($(COOH)_2$), formic acid (HCOOH), and tetrabutyl ammonium hydroxide (TBAH) were purchased from the Sinopharm Chemical Reagent Co. Ltd. (Shanghai, China). KBH_4 was obtained from Tianjing Huachen Chemical Reagent Co. Ltd. (Tianjing, China). The HPLC grade acetonitrile (ACN) was obtained from Tedia (Fairfield, U.S.A.). Sodium selenite (Se^{IV}), sodium selenate (Se^{VI}), seleno-DL-cystine ($(SeCys)_2$), seleno-DL-methionine (SeMet), and trypsin (proteomics grade) were all purchased from Sigma-Aldrich (St. Louis, MO, U.S.A.). ^{77}Se powder (99.66%) was purchased from Cambridge Isotope Laboratories, Inc. (Andover, MA, U.S.A.). All other reagents used were purchased from the Sinopharm Chemical Reagent Co. Ltd. unless stated. The stock solutions (1 mg mL^{-1}) of Se^{IV}, Se^{VI}, and SeMet were prepared, respectively, by dissolving an appropriate amount of the corresponding compound in UPW. $(SeCys)_2$ stock solution (1 mg mL^{-1}) was prepared in 0.2 mol L^{-1} HCl. The enriched isotope solution of ^{77}Se was prepared by dissolving approximately 2 mg of enriched ^{77}Se powder in high-purity grade nitric acid, and then it was diluted to 100 mL with UPW as a stock solution (2.66 μg mL^{-1}, determined by reverse isotope dilution ICPMS). Selenium-enriched yeast was obtained from Alltech Co. Ltd. (Beijing, China).

Instrumentation. Chromatographic separations were all carried out on a Shimadzu LC-2010A liquid chromatographic system (Kyoto, Japan) using a Shim-pack VP-ODS column (250 mm in length × 4.6 mm i.d., particle size 6 μm). The gradient elution was performed as 0−8 min 100% mobile phase A (3 mmol L^{-1} TBAH, 4 mmol L^{-1} $(COOH)_2$, and 2% ACN, pH 3.5) and 8−45 min 100% mobile phase B (3 mmol L^{-1} TBAH, 4 mmol L^{-1} $(COOH)_2$, and 2% ACN, pH 7.5). The flow rate of the mobile phase was 0.5 mL min^{-1}. A model AFS-610A nondispersive atomic fluorescence spectrometer (Beijing Rayleigh Analytical Instrument Co. Ltd., Beijing, China) equipped with a high-intensity Se hollow cathode lamp (196.0 nm, Beijing Shuguangming Electronic Lighting Instrument Co. Ltd., Beijing, China) was employed in this study, and signal acquisition and processing were carried out using HWH software version 1.0.[20] An ELAN DRC II ICPMS (Perkin-Elmer, SCIEX, Canada) was also used in this study. A master compact/low flow peristaltic pump (Cole-Parmer, U.S.A.) was used to introduce HCOOH into the PCVG systems. All gas chromatography/mass spectrometry (GC/MS) analysis was performed on a GC/MS-QP2010 (Shimadzu, Kyoto, Japan)

dx.doi.org/10.1021/ac3001995 | Anal. Chem. 2012, 84, 2974−2981

equipped with an electron impact ion source. Se species via flow injection (FI) or in the HPLC effluent passed through the PCVG device (Figure 1a) for VG. After gas−liquid phase

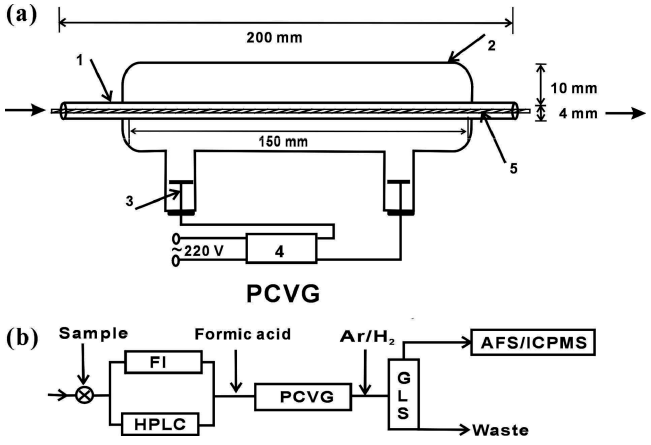

Figure 1. Schematic diagrams of the experimental system. Nanosemiconductor-based PCVG device (a): 1, central channel (200 mm in length × 4 mm o.d. × 1 mm i.d.); 2, low-pressure mercury lamp; 3, electrode; 4, electronic ballast; 5, nanosemiconductor-coated glass fiber (0.3 mm o.d.; nanosemiconductor layer thickness, 400 nm); FI/HPLC−PCVG−AFS/ICPMS system (b): FI, flow injection; GLS, gas−liquid phase separator.

separation, the generated Se volatile species were carried by argon gas into the AFS or ICPMS. A schematic diagram is shown in Figure 1b, and optimum instrumental parameters are listed in Table 1.

Nanosemiconductor-Based PCVG Device. Nano-TiO_2, ZrO_2, and the noble metal (Ag, Au, and Pt) loaded TiO_2 were prepared using the conventional sol−gel method.[4,21] Briefly, pure TiO_2 sol was prepared by mixing appropriate amounts of $Ti(OC_4H_9)_4$ and acetylacetone in ethanol (pH 3.5, adjusted with dilute HCl). After stirring for 2 h, the sol was aged for 24 h at ambient temperature. The preparation of ZrO_2 sol was similar to that of TiO_2 by mixing $Zr(OC_3H_7)_4$ and acetylacetone in ethanol. $AgNO_3$, $HAuCl_4{\cdot}3H_2O$, and $H_2PtCl_6{\cdot}6H_2O$ were added into the prepared sol solution of TiO_2. After stirring for 30 min, the sol solutions were aged for 2 h at ambient temperature. Each bare glass fiber (200 mm in length × 0.3 mm o.d., which had been washed in UPW, acetone, UPW, chromic mixture (5% chromate in H_2SO_4), and UPW in sequence, and then dried before use) was dipped into the prepared sol solution for 30 s and then slowly pulled out (repeated three times). Subsequently, the impregnated glass fiber was dried at 80 °C for 0.5 h in an electric stove. Finally, the glass fibers were put into an electric furnace and calcined at a gradually increasing temperature (1.5 °C min^{-1}) to 450 °C for TiO_2 and Ag-, Au-, and Pt-loaded TiO_2 or 600 °C for ZrO_2, before keeping that temperature for 1 h so as to obtain nano-TiO_2, Ag−TiO_2, Au−TiO_2, and Pt−TiO_2 as well as nano-ZrO_2-coated glass fibers. Scanning electron microscopy (SEM) imagines indicated that the diameters of TiO_2 and ZrO_2 particles obtained were about 10 nm; the average particle size of the noble metal was 25−70 nm, and the thickness of the three semiconductor layers was about 400 nm (Figure 2).

The prepared nanosemiconductor-coated glass fiber was inserted into the central channel of a 10 W low-pressure mercury lamp (reference designed by ourselves[22] and made by Heraeus Noblelight Ltd., Shenyang, China). It was fixed into

Table 1. Optimum Parameters for the HPLC−PCVG−AFS/ICPMS Systems

HPLC Parameters	
mobile phase A	3 mmol L^{-1} TBAH, 4 mmol L^{-1} $(COOH)_2$, 2% ACN, pH 3.5
mobile phase B	3 mmol L^{-1} TBAH, 4 mmol L^{-1} $(COOH)_2$, 2% ACN, pH 7.5
flow rate	0.5 mL min^{-1}
gradient program	0−8 min 100% A; 8−45 min 100% B
sample volume	100 μL
AFS Parameters	
PMT voltage	−310 V
HCL current	110 mA
auxiliary current	40 mA
resonance wavelength	196.0 nm
argon flow rate	400 mL min^{-1}
hydrogen flow rate	40 mL min^{-1}
ICPMS Parameters	
ICPMS	ELAN DRC II
rf power	1100 W
plasma gas flow rate	15 L min^{-1}
auxiliary gas flow rate	1.2 L min^{-1}
nebulizer gas flow rate	0.92 L min^{-1}
isotope monitored	^{82}Se
Photocatalytic Reduction Parameters	
UV lamp	10 W
photocatalyst	Ag (0.5%)/TiO_2 or ZrO_2
HCOOH concn	5% (v/v), pH 2.6
formic acid flow rate	0.3 mL min^{-1}
UV irradiation time	12 s

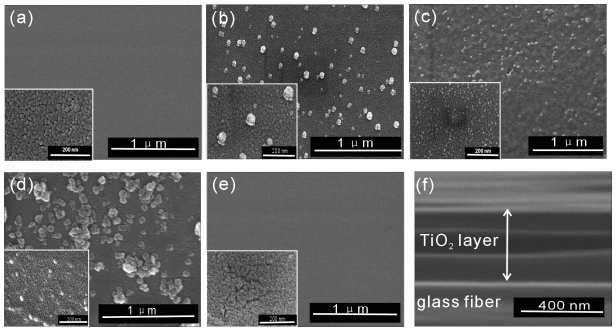

Figure 2. SEM images of the nanosemiconductor films: (a) TiO_2, (b) 0.5% Ag−TiO_2, (c) 1% Au−TiO_2, (d) 1% Pt−TiO_2, (e) ZrO_2, and (f) cross section of nano-TiO_2 layer on the surface of the glass fiber.

the central channel using a septum at each end. This nanosemiconductor-based PCVG device had a dead volume of 157 μL (Figure 1a). Considering the total flow rate of 0.8 mL min^{-1} (0.5 mL min^{-1} of the mobile phase and 0.3 mL min^{-1} of HCOOH inlet), the UV irradiation time was 12 s. The low-pressure mercury lamp mainly emitted UV light at 253.7 and 184.9 nm, which was powerful enough (4.9 and 6.7 eV) to excite the nano-TiO_2 or noble metal loaded TiO_2 (the energy gap is 3.2 eV) and nano-ZrO_2 (5.0 eV) coated on the surface of the glass fibers to generate conduction band e^-. The low-pressure mercury lamp was wrapped in aluminum foil as a light reflector for efficient irradiation and protection of the operator from ultraviolet light. The generation efficiency of the nanosemiconductor-based PCVG was estimated by comparing the signal intensity (peak area) with that obtained for the Se^{IV}

dx.doi.org/10.1021/ac3001995 | Anal. Chem. 2012, 84, 2974−2981

in the optimized conventional KBH_4−HG system (2% KBH_4 in 0.5% NaOH, 2 mol L^{-1} HCl) under the same AFS conditions.[4,9]

Sample Preparation. A microwave-assisted digestion method using an MK-III optical fiber pressure-controlled microwave decomposition system (Shinco, Shanghai, China) with 10 mL 66% HNO_3 and 2 mL 30% H_2O_2 was employed for total Se determination in selenium-enriched yeast certified reference material (CRM) SELM-1 (National Research Council of Canada, Ottawa, Canada) and the selenium-enriched yeast sample. In the case of the Se speciation analysis, two extraction methods were used for the extraction of Se species in the selenium-enriched yeast sample, whereas the recommended pretreatment method was used for SELM-1.[23] First, water extraction, where 0.1 g of the selenium-enriched yeast was transferred into a 50 mL polyethylene centrifuge tube, and then 10 mL UPW was added. The sample was then shaken at room temperature (25 ± 1 °C) for 24 h. In the case of enzymatic extraction, 0.02 g of the selenium-enriched yeast was mixed with 0.005 g of trypsin in 2.5 mL of Tris−HCl buffer solution (pH 7.5). The sample was then shaken at 37 °C for 24 h. After centrifugation for 30 min at 3000 rpm, the supernatants were decanted and filtered through a 0.45 μm membrane filter to obtain the water-extractable fraction and enzyme-extractable fraction, respectively. They were stored at 4 °C for further use.

RESULTS AND DISCUSSION

Photocatalytic Reduction Based on Noble Metal Loaded TiO_2. The PCVG efficiencies of Se^{IV} and Se^{VI} on nano-TiO_2, Ag−TiO_2, Au−TiO_2, and Pt−TiO_2 coated glass fibers under UV irradiation were determined using AFS with FI mode. The results obtained are illustrated in Figure 3,

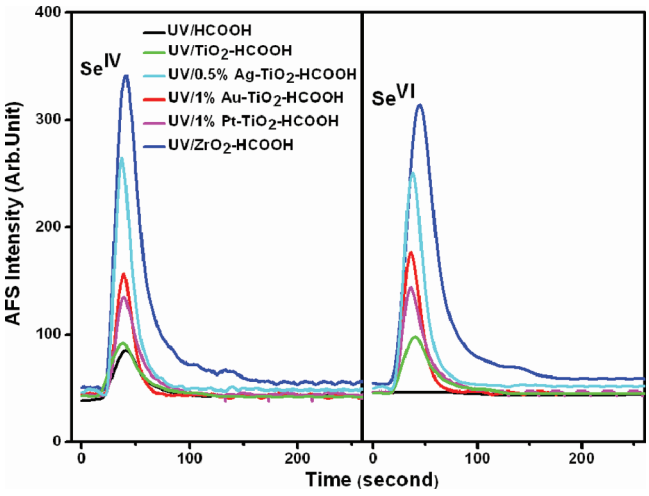

Figure 3. AFS intensities of Se^{IV} (a) and Se^{VI} (b) in different PCVG systems under FI mode. Detailed experimental conditions are listed in Table 1.

suggesting that not only both Se^{IV} and Se^{VI} can be reduced and converted directly into volatile chemical species in the nanosemiconductor-based PCVG systems but also the loading of a noble metal onto the surface of nano-TiO_2 remarkably enhanced the PCVG efficiency. According to thermodynamic data of $E^0_{SeO_4^{2-}/HSeO_3^-}$ = 1.075 V (vs NHE), $E^0_{SeO_4^{2-}/Se^0}$ = 0.876 V, $E^0_{HSeO_3^-/Se^0}$ = 0.778 V, and $E^0_{Se^0/H_2Se}$ = −0.40 V,[24,25] Se^{IV} and Se^{VI} can be reduced spontaneously by the conduction band e^- (−0.05 V at pH 0)[26] into Se^0. After all of Se^{IV} and Se^{VI} are fast reduced, the extra conduction band e^- left in the system enables the self-reduction of Se^0 to H_2Se ($Se^0 + 2H^+ + 2e^- \rightarrow H_2Se$).[27,28] Moreover, because of the higher work functions of the noble metals (φ_{Ag} = 4.26 eV, φ_{Au} = 5.1 eV, and φ_{Pt} = 5.65 eV) than that of TiO_2 (φ_{TiO_2} = 3.9 eV),[29,30] the conduction band e^- can spontaneously transfer from TiO_2 to the noble metal loaded onto nano-TiO_2 until there is an equilibrium attained between TiO_2 and the noble metal. This process causes the Fermi level of TiO_2 to shift to a more negative potential because of better e^-/h^+ separation and thus more accumulation of e^- on the conduction band. The mediation of e^- from TiO_2 to Se^0 via the noble metal accelerates the self-reduction of Se^0 to H_2Se (Scheme 1a).[31]

Scheme 1. Mechanisms in the Noble Metal Loaded TiO_2-Based (a) and ZrO_2-Based (b) PCVG Systems in the Presence of HCOOH as an h^+ Scavenger[a]

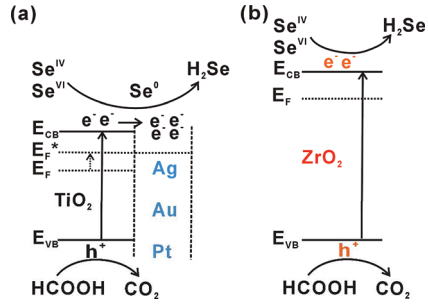

[a] E_{CB}, conduction band; E_{VB}, valence band; E_F, Fermi level.

The PCVG efficiencies of both Se^{IV} and Se^{VI} were in the order of UV/0.5%Ag−TiO_2−HCOOH (44% for Se^{IV} and 40% for Se^{VI}), UV/1.0%Au−TiO_2−HCOOH (34% and 35%), UV/1.0%Pt−TiO_2−HCOOH (26% and 28%), and UV/TiO_2−HCOOH (9% and 9%) under only 12 s of UV irradiation in the presence of 5% (v/v) HCOOH (pH 2.6) (Table 1 and Supporting Information Figures S1−S5). The reason for the higher PCVG efficiency obtained in UV/Ag−TiO_2−HCOOH over Au- or Pt-loaded systems might be due to that Ag discharged e^- more easily (lower work function) compared with Au and Pt.[32] It should be noted that the PCVG efficiency of Se species was evaluated by the comparison with the HG efficiency of Se^{IV} obtained in the most popular and conventional THB-HG system,[4,9] and the HG efficiency of Se^{IV} was a function of the concentrations of KBH_4 and HCl used in the THB-HG system. The PCVG efficiency of Se^{IV} was lower than that obtained in the THB-HG system when 2% KBH_4 and 2 mol L^{-1} HCl were employed, but it (241.4%) was much higher than that obtained in the THB-HG system when using 0.5% KBH_4 and 1 mol L^{-1} HCl.[7] Besides, Se^{VI} could be reduced and converted directly into volatile chemical species in these nanosemiconductor-based PCVG systems without using any other reducing agents such as THB, thus overcoming the problem encountered in the THB-HG system whereby Se^{VI} could not be directly converted into volatile H_2Se, and the PCVG efficiency of Se^{VI} reached 206.7% evaluated by comparison with that of Se^{IV} obtained in the THB-VG system when using 0.5% KBH_4 and 1 mol L^{-1} HCl.[7] In the cases of SeMet and $(SeCys)_2$, the UV light at 253.7 nm (4.9 eV, corresponding to 471 kJ mol^{-1}) and 184.9 nm (6.7 eV, 647 kJ

dx.doi.org/10.1021/ac3001995 | Anal. Chem. 2012, 84, 2974−2981

mol^{-1}) emitted from the low-pressure mercury lamp was powerful enough to cleave the bonds between C−Se (bond energy, 590.4 ± 4.9 kJ mol^{-1}) and Se−Se (330.5 kJ mol^{-1}) in SeMet and $(SeCys)_2$,[33] and thus reduced by the conduction band e^- into H_2Se. Their PCVG efficiencies were 43% and 9% in UV/0.5%Ag−TiO_2−HCOOH when compared with that of Se^{IV} obtained in the THB-HG system when 2% KBH_4 and 2 mol L^{-1} HCl were employed. The PCVG efficiency of 43% for SeMet obtained in UV/0.5%Ag−TiO_2−HCOOH with only 12 s of UV irradiation was much higher than that reported in UV/HCOOH system under the UV irradiation of about 2 min when considering that the VG efficiency of SeMet was half that of Se^{IV} (10−15%).[9,12]

Photocatalytic Reduction Based on Nano-ZrO_2. ZrO_2 was associated with higher negative potential conduction band e^- (−1.0 V at pH 0)[34] compared to TiO_2 (−0.05 V at pH 0). It was negative enough compared with the redox potential $E^0_{Se^0/H_2Se}$ = −0.40 V to reduce Se^{IV} and Se^{VI} directly into H_2Se across the Se self-reduction step that occurred in the UV/Ag−TiO_2−HCOOH system (Scheme 1b). The PCVG efficiencies of Se^{IV} and Se^{VI} in the UV/ZrO_2−HCOOH system were studied in a similar manner to those in the TiO_2-based systems. The results obtained indicated that not only Se^{IV} and Se^{VI} (Figure 2) but also SeMet and $(SeCys)_2$ can be converted directly into volatile species. The PCVG efficiencies of Se^{IV}, Se^{VI}, SeMet, and $(SeCys)_2$ were much higher than those obtained in the UV/Ag−TiO_2−HCOOH system and reached 70%, 60%, 68%, and 14%, respectively, when compared with that of Se^{IV} obtained in the THB-HG using 2% KBH_4 and 2 mol L^{-1} HCl, demonstrating that UV/ZrO_2−HCOOH is a more effective PCVG system.

The reaction of aqueous THB with organoselenium compounds produced volatile species such as dimethylselenide, dimethyldiselenide, diethyldiselenide, and ethylhydrogenselenide depending on the kind of organoselenium species such as selenomethionine, selenoethionine, and trimethylselenonium;[35] and especially, when using UV/HCOOH system to reduce Se species into volatile species, both of H_2Se and SeCO were identified and the ratio of them was a function of the composition of the reaction medium.[9] In order to distinguish the volatile Se species generated and understand the reduction mechanisms in the UV/Ag−TiO_2−HCOOH and UV/ZrO_2−HCOOH systems, the volatile Se species generated from Se^{IV}, Se^{VI}, SeMet, and $(SeCys)_2$ were first swept into 0.005 mol L^{-1} $CuSO_4$ and then 0.1 mol L^{-1} NaOH solutions by argon gas, and finally transferred into the AFS (see details in Supporting Information Figure S6). H_2Se could be trapped by the two solutions because it can react with $CuSO_4$ and NaOH to form CuSe (black precipitate) and Na_2Se, whereas other volatile species were generally regarded as stable to pass through the two solutions.[9,27,28] The results from AFS indicated that no Se signal was detected after the volatile Se species passed through the two solutions, suggesting that almost all the volatile Se species generated in the UV/Ag−TiO_2−HCOOH and UV/ZrO_2−HCOOH systems was H_2Se. Moreover, ^{77}Se-enriched Se^{IV} (1 μg mL^{-1}) was also employed and reduced in the UV/Ag−TiO_2−HCOOH and/or UV/ZrO_2−HCOOH systems. The volatile Se species generated were cryogenically trapped by liquid nitrogen (−196 °C, see details in Supporting Information Figure S7) and identified by GC/MS.[9] Peaks corresponding to $H_2{}^{77}Se^+$ at m/z 79, $H^{77}Se^+$ 78, and $^{77}Se^+$ 77 were observed in the mass spectrum when using an electron impact ion source (Figure 4). This observation further confirmed that H_2Se was generated rather than other volatile Se species in the nanosemiconductor-based PCVG systems. Different from the UV/HCOOH system without any catalysts, in which volatile SeCO was generated together with H_2Se, only H_2Se was generated in the UV/Ag−TiO_2−HCOOH and/or UV/ZrO_2−HCOOH systems. HCOOH was the precursor of reductive radicals in the UV/HCOOH system,[9] whereas it served dominantly as a valence band h^+ scavenger via its reaction with the h^+ in both the UV/Ag−TiO_2−HCOOH and/or UV/ZrO_2−HCOOH systems. HCOOH and its radicals might be oxidized directly into CO_2 prior to that they reacted with Se species because of the very strong oxidation ability of the h^+ (3.2 (TiO_2)[26] and 4.0 V (ZrO_2)[34]) generated in the two PCVG systems. This prior process led to a very efficient h^+ scavenging and a significant prevention of the recombination of e^-/h^+ pairs and, thus, resulted in a bumper conduction band e^- harvest, improving the reduction of Se species and their PCVG efficiencies.

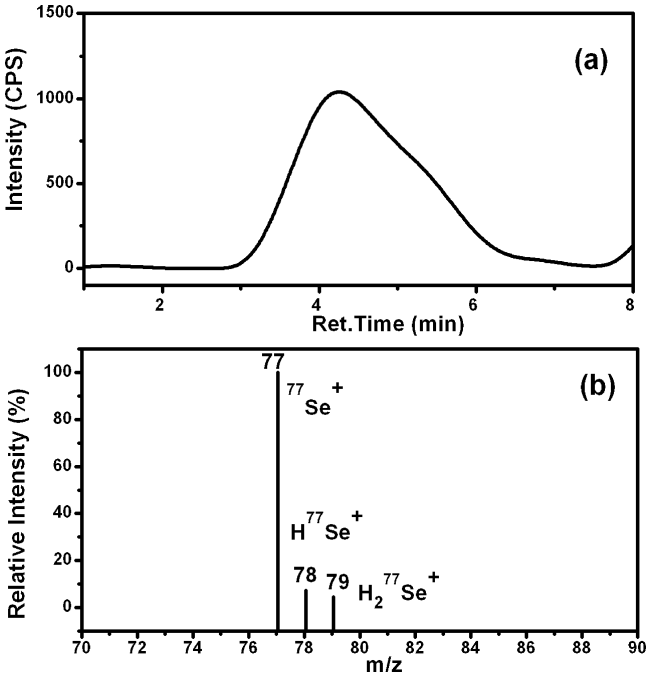

Figure 4. Typical mass spectra of the cryogenically trapped volatile Se species generated in the UV/Ag−TiO_2−HCOOH and/or UV/ZrO_2−HCOOH systems. The total ion chromatogram (a); the mass spectrum extracted from the chromatographic peak in Figure 3a (b). Column, Rtx-5 ms capillary column (30 m in length × 0.25 mm i.d. × 0.25 mm film); injection volume, 500 μL; injection temperature, 150 °C; oven temperature, 35 °C (isothermal); carrier gas (He) flow rate, 5.0 mL min^{-1}; electron impact ion source, 70 eV.

Analytical Performance and Applications. Limits of detection (LODs, 3σ) of Se^{IV}, Se^{VI}, $(SeCys)_2$, and SeMet were 1.2, 1.8, 7.4, and 0.9 ng mL^{-1} in the UV/Ag−TiO_2−HCOOH system and 0.7, 1.0, 4.2, and 0.5 ng mL^{-1} in the UV/ZrO_2−HCOOH system using AFS under FI mode. The linear range of their calibration curves was from 0 to 5 μg mL^{-1} with regression coefficients (R^2) greater than 0.993. The relative standard deviations (RSDs) of the four Se species were less than 5.1% (n = 9 at 1 μg mL^{-1}). When using ICPMS, the LODs (3σ) of the four typical Se species reached 10, 14, 18, and 8 pg mL^{-1} in UV/Ag−TiO_2−HCOOH, and 6, 7, 10, and 5 pg mL^{-1} in UV/ZrO_2−HCOOH with the RSDs lower than 4.4% (n = 9 at 10 ng mL^{-1}). Clearly, not only Se^{IV}, SeMet, and

dx.doi.org/10.1021/ac3001995 | Anal. Chem. 2012, 84, 2974−2981

$(SeCys)_2$ were reduced efficiently into volatile Se species in both the UV/Ag–TiO_2–HCOOH and UV/ZrO_2–HCOOH PCVG systems as in the THB-HG system,[35−37] but also Se^{VI} could be converted efficiently and directly into H_2Se in the two PCVG systems without any additional prereduction procedures.

Besides, both UV/Ag–TiO_2–HCOOH and UV/ZrO_2–HCOOH PCVG devices were used as interfaces between HPLC and AFS or ICPMS for Se speciation analysis (Figures 5 and 6). Mutual separation of the Se species (Se^{IV}, Se^{VI}, $(SeCys)_2$, and SeMet) was performed using an ion-pair RP-HPLC system.[38] Typical chromatograms of Se^{IV}, Se^{VI}, $(SeCys)_2$, and SeMet obtained using HPLC–(UV/Ag–TiO_2)–AFS/ICPMS and HPLC–(UV/ZrO_2)–AFS/ICPMS are shown in Figure 5, parts a and b, and Figure 6, parts a and b. A comparison of the LODs of the Se species obtained using the methods developed in this study with those reported in the literature is given in Table 2, suggesting that the methods developed in this study are sensitive and practical for Se determination and speciation analysis. Especially in the cases of HPLC–(UV/Ag–TiO_2)–ICPMS and HPLC–(UV/ZrO_2)–ICPMS, they are the most sensitive ones reported so far.

Before applying HPLC–(UV/Ag–TiO_2)–AFS, HPLC–(UV/Ag–TiO_2)–ICPMS, HPLC–(UV/ZrO_2)–AFS, and HPLC–(UV/ZrO_2)–ICPMS to Se speciation analysis, they were first validated using a water standard reference material (SRM) GBW(E)080395 (National Research Centre for Certified Reference Materials, Beijing, China). The average

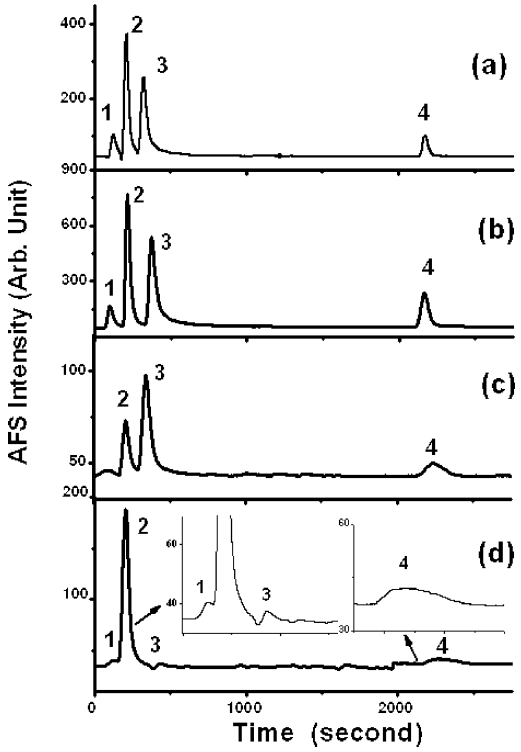

Figure 5. Typical chromatograms of a mixture containing $(SeCys)_2$, SeMet, Se^{IV}, and Se^{VI} of 1 μg mL^{-1} each, using HPLC–(UV/Ag–TiO_2)–AFS (a) and HPLC–(UV/ZrO_2)–AFS (b); Se speciation in the water-extractable fraction (c) and the enzyme-extractable fraction (d) of the selenium-enriched yeast sample using HPLC–(UV/ZrO_2)–AFS. 1, $(SeCys)_2$; 2, SeMet; 3, Se^{IV}; 4, Se^{VI}. Detailed experimental conditions are listed in Table 1.

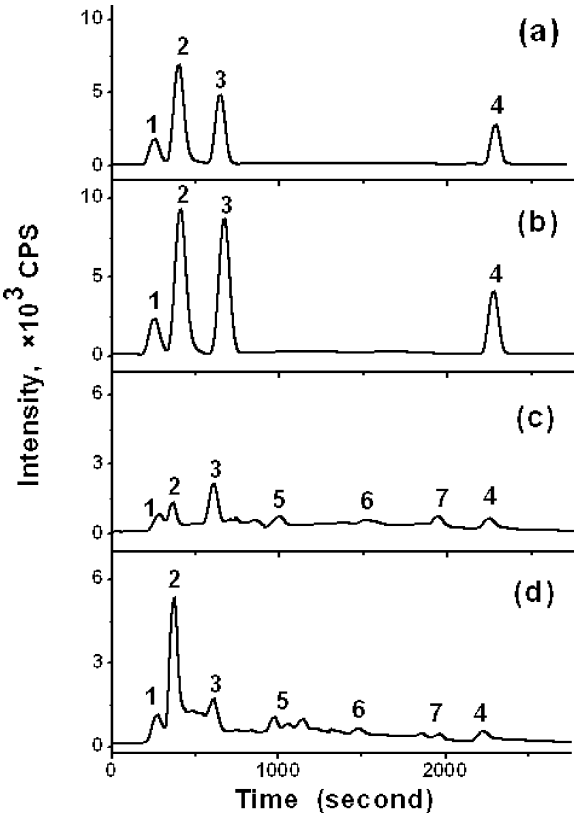

Figure 6. Typical chromatograms of a mixture containing $(SeCys)_2$, SeMet, Se^{IV}, and Se^{VI} of 100 ng mL^{-1} each, using HPLC–(UV/Ag–TiO_2)–ICPMS (a) and HPLC–(UV/ZrO_2)–ICPMS (b); Se speciation in the water-extractable fraction (c) and the enzyme-extractable fraction (d) of the selenium-enriched yeast sample using HPLC–(UV/ZrO_2)–ICPMS. 1, $(SeCys)_2$; 2, SeMet; 3, Se^{IV}; 4, Se^{VI}; 5–7, unknown Se species. Detailed experimental conditions are listed in Table 1.

Table 2. Comparison of the LODs (ng mL^{-1}) Obtained Using the Methods Developed in This Study with Those Reported in the Literature

analytical techniques[a]	Se^{IV}	Se^{VI}	$(SeCys)_2$	SeMet	ref
HPLC–UV/Ag–TiO_2–AFS	3.6	7.6	10.9	2.3	this study
HPLC–UV/ZrO_2–AFS	1.9	3.9	6.8	1.3	this study
HPLC–UV/Ag–TiO_2–ICPMS	0.024	0.023	0.029	0.014	this study
HPLC–UV/ZrO_2–ICPMS	0.014	0.016	0.018	0.007	this study
HPLC–HG–AFS	16		70	18	39
HPLC–UV–HG–AFS	2.3	5.7	9	4.3	40
HPLC–UV/TiO_2–ECVG–AFS	2.9	3.5	2.1	4.3	5
HPLC–UV/TiO_2–HG–AFS	6.7	10.3	5.4	25.9	4
HPLC–ICPMS	1.8	2.6	2.3	1.7	41
HPLC–MW–HG–ICPMS	4.4	2.0	1.2	0.7	42
HPLC–UV/TiO_2–ICPMS	0.060	0.030			7

[a]HG, THB-HG; ECVG, electrochemical chemical vapor generation; MW, microwave.

dx.doi.org/10.1021/ac3001995 | Anal. Chem. 2012, 84, 2974–2981

Table 3. Selenium Determination and Speciation of CRM SELM-1 and the Selenium-Enriched Yeast Sample (μg Se g^{-1}, n = 3)

	CRM SELM-1				
	certified value	HPLC−UV/Ag−TiO_2−AFS	HPLC−UV/ZrO_2−AFS	HPLC−UV/Ag−TiO_2−ICPMS	HPLC−UV/ZrO_2−ICPMS
SeMet	3389 ± 173[a]	3328 ± 122[a]	3357 ± 69[a]	3361 ± 62[a]	3324 ± 37[a]
total Se	2059 ± 64	2027 ± 74	2045 ± 38	2055 ± 33	2033 ± 42

	Selenium-Enriched Yeast Sample							
	HPLC−UV/Ag−TiO_2−AFS		HPLC−UV/ZrO_2−AFS		HPLC−UV/Ag−TiO_2−ICPMS		HPLC−UV/ZrO_2−ICPMS	
	water extract	enzymatic extract	water extract	enzymatic extract	water extract	enzymatic extract	water extract	enzymatic extract
SeMet	159.3 ± 0.8	857.6 ± 1.7	157.9 ± 0.6	866.5 ± 3.4	161.5 ± 1.1	894.2 ± 2.3	160.9 ± 1.6	891.0 ± 2.7
$(SeCys)_2$	N.D.[b]	52.4 ± 1.2	N.D.[b]	53.2 ± 0.8	27.5 ± 0.7	54.3 ± 1.2	26.7 ± 0.6	53.2 ± 0.8
Se^{IV}	44.9 ± 0.5	67.2 ± 0.5	43.1 ± 1.6	67.0 ± 1.9	42.1 ± 0.7	66.8 ± 0.9	47.1 ± 1.6	67.6 ±1.1
Se^{VI}	33.2 ± 0.8	51.7 ± 0.7	30.1 ± 1.3	47.1 ± 0.9	32.8 ± 0.8	52.6 ± 0.6	33.4 ± 1.2	50.9 ± 0.6
extractable Se	237.4 ± 2.1	1027.3 ± 4.1	231.2 ± 3.5	1043.8 ± 6.0	263.9 ± 3.3	1067.9 ± 4.4	268.1 ± 2.5	1058.7 ± 5.0
total Se	1999 ± 26		1998 ± 20		2006 ± 35		2003 ± 24	

[a] μg SeMet g^{-1}. [b] Not detected.

value determined (998 ± 65 ng Se mL^{-1}, n = 3 for each system) was well in agreement with the certified value (1000 ± 90 ng mL^{-1}). They were also validated using selenium-enriched yeast certified reference material SELM-1. The extraction process for the speciation of selenium in SELM-1 was based on the method recommended by McSheehy et al.[23] The results obtained are listed in Table 3. They were well in accordance with the certified values of total Se and SeMet, indicating the accuracy of these methods developed again. Finally, they were applied to the determination of the total Se content in the selenium-enriched yeast sample purchased from Alltech Co. Ltd. and Se speciation in the water-extractable and enzyme-extractable fractions of the selenium-enriched yeast. The results obtained are listed Table 3, and typical chromatograms of Se speciation in both the extractable fractions of the selenium-enriched yeast are shown in Figure 5, parts c and d (when using HPLC−(UV/ZrO_2)−AFS), and Figure 6, parts c and d (HPLC−(UV/ZrO_2)−ICPMS). The results obtained clearly indicated that the enzymatic extraction efficiencies (51−53%) were more efficient than those (11−13%) of the water extraction method. Besides Se^{IV}, Se^{VI}, $(SeCys)_2$, and SeMet, several unknown Se species were determined in both the water- and enzyme-extractable fractions of the selenium-enriched yeast when using more sensitive ICPMS (Figure 6, parts c and d). The unknown Se species needed to be further identified. Among the Se species determined, SeMet accounted for 60−68% of the water-extractable Se and 83−84% of enzyme-extractable Se when they were expressed as μg Se g^{-1}, suggesting that SeMet was dominantly presented in the selenium-enriched yeast.[43,44]

CONCLUSIONS

The UV/Ag−TiO_2−HCOOH and UV/ZrO_2−HCOOH PCVG systems developed in this study were effective for direct VG of the four typical Se species without the aid of any additional reductants. Especially, the two PCVG systems significantly improved the VG efficiency of Se^{VI} compared with those reported in the conventional THB-HG and low molecular weight organic acid-based photoinduced as well as TiO_2-based photocatalytic VG systems. Furthermore, the two PCVG systems were able to apply for the effective VG of SeMet and $(SeCys)_2$. The PCVG systems were used not only as highly efficient sample introduction systems for subsequent high-sensitivity atomic spectrometric determination of Se but also as interfaces between HPLC and element-specific detectors (such as AFS and ICPMS) for Se speciation analysis. Not simply limited to the Se studied here, the two PCVG systems are expected to be applicable to the high-sensitivity determination and speciation of other vapor-generable elements such as mercury, arsenic, antimony, etc. in the near future to offer accurate information when their environmental behavior and biological effect are evaluated.

ASSOCIATED CONTENT

Supporting Information

Additional information as noted in text. This material is available free of charge via the Internet at http://pubs.acs.org.

AUTHOR INFORMATION

Corresponding Author

*E-mail: qqwang@xmu.edu.cn.

Notes

The authors declare no competing financial interest.

ACKNOWLEDGMENTS

This study was financially supported by the National Natural Science Foundation of China (21035006) and the National Basic Research 973 Program (2009CB421605). We thank Professor John Hodgkiss for his help with the English.

REFERENCES

(1) Holak, W. *Anal. Chem.* **1969**, *41*, 1712−1713.
(2) Braman, R. S.; Justen, L. L.; Foreback, C. C. *Anal. Chem.* **1972**, *44*, 2195−2199.
(3) D'Ulivo, A.; Dedina, J.; Mester, Z.; Sturgeon, R. E.; Wang, Q. Q.; Welz, B. *Pure Appl. Chem.* **2011**, *83*, 1283−1340.
(4) Wang, Q. Q.; Liang, J.; Qiu, J. H.; Huang, B. L. *J. Anal. At. Spectrom.* **2004**, *19*, 715−716.
(5) Liang, J.; Wang, Q. Q.; Huang, B. L. *Anal. Bioanal. Chem.* **2005**, *381*, 366−372.
(6) Yin, Y. M.; Liang, J.; Yang, L. M.; Wang, Q. Q. *J. Anal. At. Spectrom.* **2007**, *22*, 330−334.
(7) Sun, Y. C.; Chang, Y. C.; Su, C. K. *Anal. Chem.* **2006**, *78*, 2640−2645.
(8) Zheng, C. B.; Wu, L.; Ma, Q.; Lv, Y.; Hou, X. D. *J. Anal. At. Spectrom.* **2008**, *23*, 514−520.
(9) Guo, X. M.; Sturgeon, R. E.; Mester, Z.; Gardner, G. J. *Anal. Chem.* **2003**, *75*, 2092−2099.
(10) Guo, X. M.; Sturgeon, R. E.; Mester, Z.; Gardner, G. J. *Anal. Chem.* **2004**, *76*, 2401−2405.

(11) Zheng, C. B.; Li, Y.; He, Y. H.; Ma, Q.; Hou, X. D. *J. Anal. At. Spectrom.* **2005**, *20*, 746−750.
(12) García, M.; Figueroa, R.; Lavilla, I.; Bendicho, C. *J. Anal. At. Spectrom.* **2006**, *21*, 582−587.
(13) Yin, Y. M.; Qiu, J. H.; Yang, L. M.; Wang, Q. Q. *Anal. Bioanal. Chem.* **2007**, *388*, 831−836.
(14) Yin, Y. G.; Liu, J. F.; He, B.; Gao, E. L.; Jiang, G. B. *J. Anal. At. Spectrom.* **2007**, *22*, 822−826.
(15) Yin, Y. G.; Liu, J. F.; He, B.; Shi, J. B.; Jiang, G. B. *J. Chromatogr., A* **2008**, *1181*, 77−82.
(16) Tang, L.; Chen, F.; Yang, L. M.; Wang, Q. Q. *J. Chromatogr., B* **2009**, *877*, 3428−3433.
(17) Zheng, C. B.; Ma, Q.; Wu, L.; Hou, X. D.; Sturgeon, R. E. *Microchem. J.* **2010**, *95*, 32−37.
(18) Yin, Y. G.; Liu, J. F.; Jiang, G. B. *TrAC, Trends Anal. Chem.* **2011**, *30*, 1672−1684.
(19) Sturgeon, R. E.; Guo, X. M.; Mester, Z. *Anal. Bioanal. Chem.* **2005**, *382*, 881−883.
(20) Hong, Y. C.; Wang, Q. Q.; Yan, H.; Liang, J.; Guo, X. M.; Huang, B. L. *Spectrosc. Spectral Anal. (Beijing)* **2003**, *23*, 354−357.
(21) Epifani, M.; Giannini, C.; Tapfer, L.; Vasanelli, L. *J. Am. Ceram. Soc.* **2000**, *83*, 2385−2393.
(22) Nakazato, T.; Tao, H. *Anal. Chem.* **2006**, *78*, 1665−1672.
(23) McSheehy, S.; Yang, L.; Sturgeon, R.; Mester, Z. *Anal. Chem.* **2005**, *77*, 344−349.
(24) Sanuki, S.; Kojima, T.; Arai, K.; Nagaoka, S.; Majima, H. *Metall. Mater. Trans. B* **1999**, *30*, 15−20.
(25) Séby, F.; Potin-Gautier, M.; Giffaut, E.; Borge, G.; Donard, O. F. X. *Chem. Geol.* **2001**, *171*, 173−194.
(26) Chen, D.; Ray, A. K. *Chem. Eng. Sci.* **2001**, *56*, 1561−1570.
(27) Tan, T. T. Y.; Zaw, M.; Beydoun, D.; Amal, R. *J. Nanopart. Res.* **2002**, *4*, 541−552.
(28) Tan, T. T. Y.; Beydoun, D.; Amal, R. *J. Mol. Catal. A: Chem.* **2003**, *202*, 73−85.
(29) Michaelson, H. B. *J. Appl. Phys.* **1977**, *48*, 4729−4733.
(30) Könenkamp, R. *Phys. Rev. B* **2000**, *61*, 11057−11064.
(31) Tan, T. T. Y.; Yip, C. K.; Beydoun, D.; Amal, R. *Chem. Eng. J.* **2003**, *95*, 179−186.
(32) E, L.; Xu, M. X. *J. Chin. Ceram. Soc.* **2004**, *32*, 1538−1541.
(33) Luo, Y. R. *Comprehensive Handbook of Chemical Band Energies*; CRC Press: Boca Raton, FL, 2007.
(34) Sayama, K.; Arakawa, H. *J. Phys. Chem.* **1993**, *97*, 531−533.
(35) Chatterjee, A.; Shibata, Y.; Yoneda, M.; Banerjee, R.; Uchida, M.; Kon, H.; Morita, M. *Anal. Chem.* **2001**, *73*, 3181−3186.
(36) Chatterjee, A.; Irgolic, K. J. *Anal. Commun.* **1998**, *35*, 337−340.
(37) Chatterjee, A.; Shibata, Y.; Morita, M. *Microchem. J.* **2001**, *69*, 179−187.
(38) Qiu, J. H.; Wang, Q. Q.; Ma, Y. N.; Yang, L. M.; Huang, B. L. *Spectrochim. Acta, Part B* **2006**, *61*, 803−809.
(39) Ipolyi, I.; Stefánka, Z.; Fodor, P. *Anal. Chim. Acta* **2001**, *435*, 367−375.
(40) González LaFuente, J. M.; Dlaska, M.; Fernández Sánchez, M. L.; Sanz-Medel, A. *J. Anal. At. Spectrom.* **1998**, *13*, 423−429.
(41) Mazej, D.; Falnoga, I.; Veber, M.; Stibilj, V. *Talanta* **2006**, *68*, 558−568.
(42) Pedersen, G. A.; Larsen, E. H. *Fresenius' J. Anal. Chem.* **1997**, *358*, 591−598.
(43) Casiot, C.; Szpunar, J.; Łobiński, R.; Potin-Gautier, M. *J. Anal. At. Spectrom.* **1999**, *14*, 645−650.
(44) Chen, B. B.; He, M.; Mao, X. J.; Cui, R.; Pang, D. W.; Hu, B. *Talanta* **2011**, *83*, 724−731.